

# QCD Properties of Hot/Dense Matter

Su Hounng Lee<sup>a\*</sup>

<sup>a</sup>Department of Physics, Yonsei University,  
Seoul 120-749, Korea

In the introduction, we will discuss the symmetries of QCD, its breaking in the physical vacuum and its restoration at finite temperature and/or density. Then we will discuss what exact relations can be made between chiral symmetry restoration and the imaginary part of the vector vector correlation function, which is directly related to the dilepton spectrum coming from a hot and/or dense medium. Finally, we will focus on the vector meson pole appearing in the imaginary part and discuss results on how the shape changes using QCD sum rules in medium. In particular, we will discuss three characteristic changes of the vector meson peaks; namely, shift of the peak position, increase of its width and the dispersion effect due to the breaking of Lorentz invariance in medium.

## 1. INTRODUCTION

At zero temperature and/or baryon density, the chiral symmetry is spontaneously broken  $\langle \bar{q}q \rangle \neq 0$  and the hadronic world has only  $SU(N)_V \times U(1)_V$  symmetry. However, if the temperature or baryon density increases, there will be a critical boundary above which the broken chiral symmetry gets restored  $\langle \bar{q}q \rangle = 0$  and the hadronic matter changes to a quark gluon plasma (QGP) state. This QGP state will have  $SU(N)_L \times SU(N)_R \times U(1)_V$  symmetry, which is also the symmetry of QCD at the quantum level.

### 1.1. Symmetry of QCD

The Lagrangian of QCD is;

$$\mathcal{L}_{QCD} = -\frac{1}{4}F_{\mu\nu}^a F_{\mu\nu}^a - \sum_f \bar{q}_f (i\not{D} + M_f) q_f \quad (1)$$

where  $F_{\mu\nu}^a = \partial_\mu A_\nu^a - \partial_\nu A_\mu^a + igf^{abc}A_\mu^b A_\nu^c$  and  $A_\mu^a$  represents the spin 1 gauge field with color index  $a$ .  $q_f$  represents the spin  $\frac{1}{2}$  matter field which has left and right chirality components,  $q_{L,R} = \frac{1}{2}(1 \mp \gamma_5)q$ , and the index  $f$  represents the  $N$  number of flavors such as the  $u, d, s \dots$ . In the chiral limit ( $M \rightarrow 0$ ),  $\mathcal{L}_{QCD}$  is symmetric under  $U(N)_L \times U(N)_R$ ,

---

\*This work was supported in part by the Korean Ministry of Education through grant no. BSRI-97-2425 and by the KOSEF through grant no. 971-0204-017-2 and the CTP at Seoul National University.

i.e., the lagrangian is symmetric under the following left right transformation.

$$\begin{pmatrix} u \\ d \\ s \\ \cdot \end{pmatrix} \rightarrow e^{iQ} \begin{pmatrix} u \\ d \\ s \\ \cdot \end{pmatrix} \quad (2)$$

where  $Q = \frac{1-\gamma_5}{2}(L_0 + L_i\lambda^i) + \frac{1+\gamma_5}{2}(R_0 + R_i\lambda^i)$ . Under this transformation, the chirality does not mix ( $q_{L,R} \rightarrow q_{L,R}$ ).

However, at the quantum level, due to the axial anomaly, the  $U_A(1)$  symmetry ( $Q = \gamma_5(R_0 - L_0)$ ) is broken and QCD is symmetric only under

$$SU(N)_L \times SU(N)_R \times U(1)_V. \quad (3)$$

This is also the symmetry of the QGP state.

### 1.2. Spontaneously broken chiral symmetry

In the hadronic world, the QCD symmetry at quantum level is further broken down spontaneously to the following group.

$$SU(N)_V \times U(1)_V \quad (4)$$

As a consequence the QCD vacuum and physical excitations are not symmetric under  $Q = \gamma_5 Q^a \lambda^a$  transformation. This is manifest from looking at various order parameters of chiral symmetry.

First, consider the vacuum state. The chiral partner of any quark composite operator  $Op$  is obtained by taking its commutator with the chiral charge operator  $F_5^a = \int d^3x \bar{q}\gamma_0\gamma^5\frac{\lambda^a}{2}q$ . Hence the chiral partner of  $\bar{q}q$  is  $\bar{q}\gamma_5\frac{\lambda^a}{2}q$ . Since the vacuum expectation value of the latter vanishes identically,  $\langle\bar{q}q\rangle \neq 0$  shows that chiral symmetry is broken in the vacuum. The fact that chiral symmetry is spontaneously broken is also manifest in the presence of massless Nambu-Goldstone Bosons ( the  $\pi$ 's), which couple to the broken axial current  $\langle 0|A_\mu^5|\pi\rangle \sim f_\pi$ .

As can be seen from table 1, the broken chiral symmetry is also manifest in the mesonic excitation, such as  $m_\rho \neq m_{a_1}$ , and baryonic excitations, such as  $m_P \neq m_{S_{11}}$  [1,2].

Table 1

Chiral order parameters and evidence for its breaking in hadronic world. Here  $V_\mu^a = \bar{q}\gamma_\mu\frac{\lambda^a}{2}q$ ,  $A_\mu^a = \bar{q}\gamma_\mu\gamma_5\frac{\lambda^a}{2}q$ .  $\Psi_-$  is the chiral partner of  $\Psi_+$ .

Order parameter	Hadronic world
$\langle\bar{q}q\rangle$	$\langle\bar{q}q\rangle \neq 0, f_\pi^2 m_\pi^2 = -\langle m\bar{q}q\rangle$
$\langle V_\mu^a(x)V_\mu^a(0)\rangle - \langle A_\mu^a(x)A_\mu^a(0)\rangle$	$m_\rho(770) \neq m_{a_1}(1250)$
$\langle\Psi_+(x)\Psi_+(0)\rangle - \langle\Psi_-(x)\Psi_-(0)\rangle$	$m_P(938) \neq m_{S_{11}}(1535)$

### 1.3. Chiral symmetry restoration at high temperature and/or density

As seen from lattice gauge theory calculations, the broken chiral symmetry will be restored at high temperature. The transition will become smooth as we increase the current quark mass. The actual order of the phase transition at the physical value of the quark masses for the  $u, d, s$  quarks are still controversial. The result using the Staggered fermions[3] shows a smooth transition at the physical value of the quark masses. However, the result using the Wilson fermions[4] shows a first order transition.

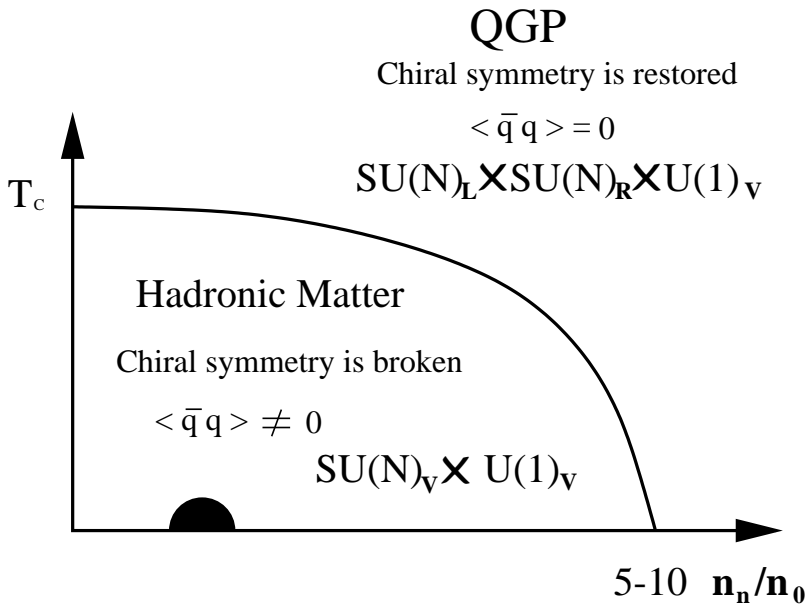


Figure 1. Phase diagram of QCD.

At present, the lattice calculation at finite density suffers a technical difficulty due to complex fermion determinant. Nevertheless, many model calculations, such as instanton models[5], NJL model, Random Matrix model[6] suggest that chiral symmetry will also be restored at finite baryon density. In fact, already at nuclear matter density, there exist model independent relations that shows that the chiral order parameter will be reduced to about 80 % of its vacuum value. Therefore, any physical effect related to chiral symmetry restoration will also be partially visible in nuclear matter.

### 1.4. $U_A(1)$ restoration at high temperature and/or density

Present lattice calculations shows that the  $U_A(1)$  symmetry is not restored above the chiral phase transition[7,8]. This is reasonable because the  $U_A(1)$  breaking effect comes from a totally different mechanism from that of chiral symmetry breaking. Nevertheless, the present lattice calculations were performed with  $N = 2$  flavors and studied the  $U_A(1)$  order parameter constructed out of two quark bilinears (2-point function). It would be interesting to perform similar calculations with larger number of flavors. The reason, which is valid above  $T_c$ , is the following. The  $U_A(1)$  breaking effect comes from topo-

logically non-trivial gauge field configurations. Its contribution to the partition function has measure zero in the chiral limit, i.e. its contribution is proportional to the  $M^N \rho_{inst}$ , where  $N$  is the number of quark flavors having current quark mass  $M$ , and  $\rho_{inst}$  is the pseudo-instanton density[9]. For  $U_A(1)$  order parameter, constructed out of  $n$  quark bilinears, the breaking contribution is proportional to  $M^{N-n} \rho_{inst}$ . This implies, that in the chiral limit, after chiral symmetry restoration, the  $U_A(1)$  breaking effect shows up only when  $n \geq N$ [10].

Table 2

$U_A(1)$  breaking operators and its breaking contribution from the partition function. Here  $\pi^a = \bar{q} \gamma_5 \frac{\lambda^a}{2} q$ ,  $\delta^a = \bar{q} \frac{\lambda^a}{2} q$ .  $N$  is the number of quark flavors with mass  $M$ .  $\rho_{inst}$  is the pseudo-instanton density.

Breaking operator	Breaking contribution
$\langle \bar{q} q \rangle$	$M^{N-1} \rho_{inst}$
$\langle \pi^a(x) \pi^a(0) \rangle - \langle \delta^a(x) \delta^a(0) \rangle$	$M^{N-2} \rho_{inst}$
n-point function	$M^{N-n} \rho_{inst}$

## 2. OBSERVING CHIRAL SYMMETRY RESTORATION

Among the order parameters of chiral symmetry restoration, such as those discussed in Table. 1, let us concentrate on the difference between the vector and axial vector two point functions. Using the dispersion relation, it can also be related to the difference between the imaginary parts.

$$\Pi_{\mu\mu}^V(q) - \Pi_{\mu\mu}^A(q) = \frac{1}{\pi} \int ds \left( \frac{\text{Im}\Pi^V(s)}{s - q^2} - \frac{\text{Im}\Pi^A(s)}{s - q^2} \right), \quad (5)$$

where,

$$\Pi_{\mu\nu}^V = \int d^4x e^{iqx} \langle V_\mu(x) V_\nu(0) \rangle, \quad \Pi_{\mu\nu}^A = \int d^4x e^{iqx} \langle A_\mu(x) A_\nu(0) \rangle. \quad (6)$$

The imaginary part of the vector correlator can be observed from the hadronic part of the cross-section  $e^+ + e^- \rightarrow \text{even } \pi$  Fig.2 (a). This has a sharp rho meson peak (770 MeV) followed by resonances, which add up like a continuum. The imaginary part of the axial correlator can be observed from the hadronic part of the decay  $\tau \rightarrow \text{odd } \pi$  Fig.2 (b). This part has the broad  $a_1$  peak (1260 MeV).

The two imaginary parts are clearly different and is one of the experimental signature that chiral symmetry is broken in the vacuum.

In the vacuum, due to current conservation and Lorentz invariance, the polarization functions in Eq. (6) has only one independent function, which is a function of the four momentum  $q^2 = \omega^2 - \mathbf{q}^2$ . At finite temperature or density, the Lorentz invariance is broken and the polarization functions will have a transverse ( $\Pi_T$ ) and a longitudinal

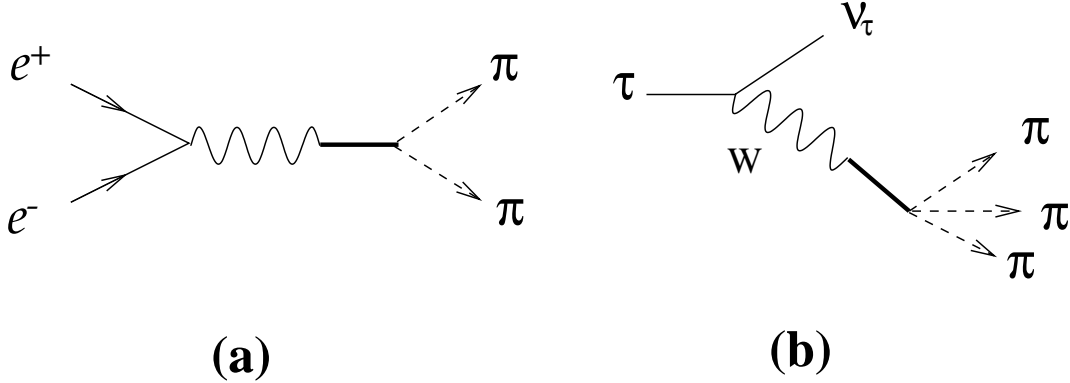


Figure 2. a)  $e^+ + e^- \rightarrow \text{even } \pi$ , b)  $\tau \rightarrow \text{odd } \pi$ .

( $\Pi_L$ ) component (with respect to  $\mathbf{q}$ ), which will depend on both the energy  $\omega$  and three momentum  $\mathbf{q}$ .

$$\Pi_{\mu\nu}(\omega, \mathbf{q}) = \Pi_T q^2 P_{\mu\nu}^T + \Pi_L q^2 P_{\mu\nu}^L, \quad (7)$$

where for  $q = (\omega, \mathbf{q})$  and medium at rest, we have,  $P_{00}^T = P_{0i}^T = P_{i0}^T = 0$ ,  $P_{ij}^T = \delta_{ij} - \mathbf{q}_i \mathbf{q}_j / \mathbf{q}^2$ , and  $P_{\mu\nu}^L = (q_\mu q_\nu / q^2 - g_{\mu\nu} - P_{\mu\nu}^T)$ .  $\Pi_L = \Pi_T$  only when  $\mathbf{q} = 0$ .

Above the critical temperature or density, chiral symmetry is restored and  $\text{Im}\Pi_{L,T}^V = \text{Im}\Pi_{L,T}^A$ , which at sufficiently high temperature or density can be calculated using perturbative QCD[11]. At high temperature or density, the poles disappear and become part of the continuum. Now the question is how would the poles behave and approach the continuum from below the critical boundary?

In fact, one can observe  $\text{Im}\Pi^V$  from a hot or dense matter by looking at the inverse process  $e^+ + e^- \rightarrow \text{even } \pi$ . That is, by looking at the dileptons coming out from the medium[12]. Since, the dileptons interact weakly in the strong interaction time scale, once they are produced, they will carry the information about  $\text{Im}\Pi^V$  directly to detectors. This would be true in the time scales involved in Relativistic Heavy Ion collisions or experiments of vector meson production inside a Heavy Nucleus planned at GSI and KEK. Unfortunately, the inverse process of  $\tau \rightarrow \text{odd } \pi$ , that is  $\tau + \nu$  coming out from the medium is not experimentally observable and one can not directly observe  $\text{Im}\Pi^A$ . So the best we can do to observe chiral symmetry restoration (at least in heavy ion collisions) is to experimentally observe  $\text{Im}\Pi^V$  (especially the characteristic changes in the peak) and do QCD model calculations to find its relation to chiral symmetry restoration.

The dilepton production rate from a hadronic system at finite temperature is given as follows.

$$\frac{dR}{dM^2} = \frac{2\alpha_{em}^2}{3\pi^2} \int dk \frac{k^2}{\omega} \frac{1}{M^2} [\text{Im}\Pi_L(\omega, k) + 2\text{Im}\Pi_T(\omega, k)] n(\omega) \quad (8)$$

where,  $\omega^2 = k^2 + M^2$  and  $n(\omega)$  is the thermal Boltzmann factor. Here,  $\text{Im}\Pi_{L,T}(\omega, k)$  is the hadronic part of the electro-magnetic vector current correlation function. If the system evolves in a RHIC, it should be folded with the evolution of the system.

Assuming no change in the hadron properties at finite temperature or density, the expected dilepton spectrum from a hot dense system will have a peak near the vector mesons. Now, if the vector mesons change their properties in medium, changes will occur in the peak. The three characteristic changes we will discuss here are, i) peak (mass) shift, ii) increased decay width, iii) dispersion effect (or finite  $\mathbf{q}$ ) effect.

### 2.1. Model calculation of $\text{Im}\Pi^V$ at finite temperature and density

Many model calculations have been performed to calculate the changes of the vector meson properties at finite temperature or density. The models are either based on effective quark lagrangian or the effective hadron lagrangian. The former approach have model dependence related to modeling the non-perturbative nature of QCD into the quark language. The latter have large model dependence in extrapolating any effective hadron lagrangian to the on shell point of the vector meson mass region. Table 3 summarizes the results of the model calculations.

Table 3

Model calculation for  $\text{Im}\Pi_V$  at finite temperature and density. The downward, upward and horizontal arrows show respectively the decreasing, increasing and little change of values.

	model	mass	width	dispersion
Finite density	Walecka model [13]	$\searrow$	$\rightarrow$	$\rightarrow$
	Quark-meson coupling model[14]	$\searrow$	$\rightarrow$	$\rightarrow$
	Phenomenological meson exchange[15]	$\searrow$	$\rightarrow$	$\rightarrow$
	Brown-Rho scaling [16]	$\searrow$	$\rightarrow$	$\rightarrow$
	$\pi - N - \Delta$ dynamics[17]	$\rightarrow$	$\nearrow$	$\rightarrow$
	$V - N - N^*$ dynamics[18]	$\rightarrow$	$\nearrow$	$\nearrow$
Finite temperature	Chiral model with Vector mesons[19,20]	$\nearrow$	$\rightarrow$	$\rightarrow$
	Chiral model with Low T theorem[21]	$\rightarrow$	$\rightarrow$	$\rightarrow$
	$\sigma$ -model with VMD[22]	$\nearrow$	$\rightarrow$	$\rightarrow$
	Hidden local symmetry[23]	$\nearrow$	$\rightarrow$	$\rightarrow$
	Collision broadening[24]	$\rightarrow$	$\nearrow$	$\rightarrow$
	Massive YM with baryons[25]	$\searrow$	$\rightarrow$	$\rightarrow$

### 2.2. QCD constraints on $\text{Im}\Pi^V$

Let us now try to construct QCD constraints on  $\text{Im}\Pi^V$  emphasizing its connection to chiral symmetry restoration. Consider either the transverse or the longitudinal polarization function in Eq.(7). The starting point is the energy dispersion relation at finite  $\mathbf{q}$ . For small  $\mathbf{q}^2 < \omega^2$ , we can make a Taylor expansion of the correlation function, which is even function of  $\omega$  and  $\mathbf{q}$ , such that,

$$\text{Re}\Pi_{L,T}(\omega, \mathbf{q}) = \text{Re} \left( \Pi^0(\omega, 0) + \Pi_{L,T}^1(\omega, 0) \mathbf{q}^2 + \dots \right)$$

$$= \frac{1}{\pi} \int_0^\infty du^2 \left( \frac{\text{Im}\Pi^0(u, 0)}{(u^2 - \omega^2)} + \frac{\text{Im}\Pi_{L,T}^1(u, 0)}{(u^2 - \omega^2)} \mathbf{q}^2 + \dots \right), \quad (9)$$

where we have assumed the retarded correlation function.

The real part of eq.(9) is calculated via the Operator Product Expansion (OPE) at large  $-\omega^2 \rightarrow \infty$  with finite  $\mathbf{q}$ . The full polarization tensor will have the following form.

$$\begin{aligned} \Pi_{\mu\nu}(\omega, \mathbf{q}) &= (q_\mu q_\nu - g_{\mu\nu}) \left[ -c_0 \ln|Q^2| + \sum_d \frac{c_{d,d}}{Q^d} A^{d,d}(n.m.) \right] \\ &+ \sum_{s,\tau=2} \frac{1}{Q^{s+\tau-2}} \left[ c_{d,\tau} g_{\mu\nu} q^{\mu_1} \dots q^{\mu_s} A_{\mu_1 \dots \mu_s}^{d,\tau}(n.m.) + \dots \right], \end{aligned} \quad (10)$$

where,  $Q^2 = \mathbf{q}^2 - \omega^2$ . Here,  $A^{d,\tau}(n.m.)$  represents the nuclear matter expectation value of an operator of dimension  $d$  and twist  $\tau = d - s$ , where  $s$  is the number of spin index. These operators are defined at the scale  $Q^2$  and the  $c$ 's are the dimensionless Wilson coefficients with the running coupling constant. This way of including the density effect is consistent at low energy[26]. The first set of terms in eq.(10) come from the OPE of scalar operators, the second set from operators with non zero spin  $s$ . From this general expression, we can extract the OPE of  $\Pi^0$ ,  $\Pi_{L,T}^1$ . Including the contribution up to dim.6 operators only, they will have the following form,

$$\begin{aligned} \Pi^0(\omega) &= \Pi_{pert}(\omega) + \frac{1}{\omega^4} b_4^0 + \frac{1}{\omega^6} b_6^0 \\ \Pi^1(\omega) &= \frac{1}{\omega^6} b_6^1 + \frac{1}{\omega^8} b_8^1 \end{aligned} \quad (11)$$

where  $b_4^0(b_6^0)$  in  $\Pi^0$  are contributions from dim.4 (dim.6) operators and  $b_6^1(b_8^1)$  in  $\Pi^1$  are from dim.4 (dim.6) operators. It should be noted that in calculating  $\Pi^1$ , it is enough to calculate only the “non-trivial”  $\mathbf{q}^2$  dependence ; i.e. neglect the dependence coming from expanding  $Q^2 = \mathbf{q}^2 - \omega^2$ . That is so because we are interested only in the Lorentz breaking effect and not in the trivial  $\mathbf{q}^2$  dependence[27]. Eq.(11) are asymptotic expansions in  $1/\omega^2$ . Looking back at the dispersion relation in Eq.(9), we can look at different moments of the imaginary part and equate it to each term in the OPE in Eq.(11).

$$\int du^2 (\text{Im}\Pi(u) - \text{Im}\Pi_{pert}(u)) u^{n-2} = -b_n \quad (12)$$

Here,  $\text{Im}\Pi(u)_{pert}$  is the corresponding imaginary part of  $\Pi_{pert}$ . For  $\text{Im}\Pi^0$ , we have 3 constraints from  $n = 2, 4, 6$  with  $b_2 = 0$ , and for  $\text{Im}\Pi^1$ , we have 3 constraints from  $n = 4, 6, 8$  with  $b_4 = 0$ ,  $\text{Im}\Pi_{pert} = 0$  for both the longitudinal and transverse directions. These constraints are model independent constraints and relates QCD perturbative calculations and expectation values of local operators to the phenomenologically observable spectral density  $\text{Im}\Pi(u)$ . The usefulness of the constraints can be summarized as follows.

1. The temperature dependence (density dependence) of the local condensates ( $b$ 's) can be calculated using lattice QCD. Therefore, starting from the vacuum form of  $\text{Im}\Pi(u)$ , one can study its changes at finite temperature or density.

2. One can look at the effect of each local operators in  $b$ 's separately. Hence, from looking at the effect of chiral symmetry breaking operators, one can study the effect of chiral symmetry restoration on  $\text{Im}\Pi(u)$ .
3. All model calculations of  $\text{Im}\Pi(u)$ , or even the experimental data itself should satisfy the above constraints.

It is straightforward to extract the chiral symmetry breaking operators. First, it should be noted that all the twist-2 and Gluonic operators, appearing in Eq.(11), are chirally symmetric operators. Four quark operators have a chirally symmetric component and a breaking part. Assuming a four quark operator  $\mathcal{O}$ , one can divide these parts by subtracting and adding its chiral partner  $\mathcal{O} = \frac{1}{2}[\mathcal{O} - \mathcal{O}(\text{chiral partner})] + \frac{1}{2}[\mathcal{O} + \mathcal{O}(\text{chiral partner})]$ . The explicit form of  $b$ 's can be found in [26] for  $\text{Im}\Pi^0$  and in [27] for  $\text{Im}\Pi^1$ . It would be extremely useful to study the temperature dependence of these chiral symmetry breaking operators on the lattice and study its phenomenological consequences using these constraints.

### 3. QCD SUM RULE RESULT FOR $\text{Im}\Pi^V$

We will now discuss specific changes of  $\text{Im}\Pi^V$  in the QCD sum rule approach.

#### 3.1. Borel sum rule for $\Pi^0$ at finite density

After the Borel transformation with respect to  $\omega$ , the dispersion relation in Eq.(9) with the OPE in Eq.(11) looks as follows.

$$\int [\text{Im}\Pi^0(u) - \text{Im}\Pi^0(u)_{\text{pert}}(u)] e^{-u^2/M^2} du^2 = \sum_{n=2,4} \frac{(-1)^{n/2+1}}{(n/2)! M^n} b_n^0 \quad (13)$$

Motivated by its form in the vacuum, the spectral density will be modeled with a pole and a continuum.

$$\text{Im}\Pi^0(u) = \frac{F\Gamma}{(u^2 - m_V^2)^2 + (m_V\Gamma)^2} + c\theta(u^2 - s_0) + \rho_{\text{scattering}} \quad (14)$$

The Borel transformation will reduce the uncertainty associated with approximating the continuum with a sharp step function. Nevertheless, it gives a maximum Borel Mass  $M_{\text{max}}^2$  above which the continuum contribution becomes too large.  $\rho_{\text{scattering}}$  is the possible subtraction constants proportional to  $\delta(u^2)$ , which can be calculated using the nucleon-hole contribution[28,29].

The next step is to calculate the changes in the condensate. We will use the linear density approximation. In this limit, the nuclear matter expectation values of any local operator  $\mathcal{O}$  can be approximated as ,

$$\langle \mathcal{O} \rangle_{n.m.} = \langle \mathcal{O} \rangle_0 + n_n \langle \mathcal{O} \rangle_N, \quad (15)$$

where  $\langle \cdot \rangle_0$  is the vacuum expectation value,  $\langle \cdot \rangle_N$  is the nucleon expectation value and  $n_n$  is the baryon density. Up to dimension 6, all the relevant expectation values appearing in



the  $\Pi^0$  sum rules are known except for the dim. 6 four quark operator, for which we will use the mean field approximation[28,29]. The truncation at dim 6 operator determines the minimum Borel mass  $M_{max}^2$ , which is determined by assuming that the power corrections are less than 30% of the perturbative contribution.

The final step is to allow the phenomenological parameters to change also in density and determine its change by making a best fit of the left hand side to the right hand side of Eq.(13) between the Borel interval  $M_{min}^2$  and  $M_{max}^2$ .

This was first applied to the vector mesons by Hatsuda and Lee [28] in the limit  $\Gamma \rightarrow 0$ . The vector meson peak was shown to shift as follows,

$$\begin{aligned} \frac{m_V(n_n)}{m_V(0)} &= 1 - (0.16 \pm 0.06) \frac{n_n}{n_0}, \\ \frac{m_\phi(n_n)}{m_\phi(0)} &= 1 - (0.03 \pm 0.015) \frac{n_n}{n_0}, \end{aligned} \quad (16)$$

where the first line denotes the result for the  $\rho$  and  $\omega$  meson and the second line that for the  $\phi$  meson.  $n_0$  denotes the nuclear saturation density. The result for the  $\rho, \omega$  meson were due mainly to the changes in the four quark condensate  $\langle(\bar{q}q)^2\rangle$  and about 30% from  $\langle\bar{q}\gamma_\mu D_\nu q\rangle$ . The former in the mean field approximation is a chiral symmetry breaking operator and the latter is a chirally symmetric operator. As for the  $\phi$  meson, the effect comes mainly from the chiral symmetry breaking operator  $\langle m_s \bar{s}s \rangle$ . Therefore, the shift in masses come mainly from chiral symmetry restoration.

Recently, the work has been extended to include possible change in the width[30]. It was found that the downward shift of the mass could be compensated by an increase in the width. Hence, there is a band of region in the mass vs. width plane where the sum rule in Eq.(13) is reasonably satisfied. However, there exist a best fit, which starting from the vacuum value changes as follows for the  $\rho, \omega$  meson,

$$\Delta m_V \sim -50 \frac{n_n}{n_0} \text{ MeV}, \quad \Delta \Gamma \sim +200 \frac{n_n}{n_0} \text{ MeV}. \quad (17)$$

Similar analysis are in progress for the  $\phi$  meson.

Summarizing the results on  $\Pi^0$ , QCD sum rule suggests that due to chiral symmetry restoration, there will be a decrease in mass and increase in the width.

### 3.2. Borel sum rule for $\Pi^1$ at finite density

As shown in Eq.(8), the dilepton spectrum will have contribution from both the longitudinal and transverse polarization function, which will now be a function of both  $\omega$  and  $\mathbf{q}$ . We will allow the parameters in Eq.(14) to vary non-trivially by a term proportional to  $\mathbf{q}^2$  and implicitly the nuclear density  $n_n$ . Such as,

$$F \rightarrow F + f \cdot \mathbf{q}^2, \quad m_V^2 \rightarrow m_V^2 + a \cdot \mathbf{q}^2, \quad S_0 \rightarrow S_0 + s \cdot \mathbf{q}^2. \quad (18)$$

In the limit  $\Gamma \rightarrow 0$ , this will give the following form for  $\text{Im}\Pi^1$ ,

$$\text{Im}\Pi^1(u) = f \cdot \delta(u^2 - m_V^2) - a \cdot F \delta'(u^2 - m_V^2) - s \cdot c_0 \delta(u^2 - S_0) + 8\pi^2 n_n b_{scatt} \delta'(u^2). \quad (19)$$

Here, we have included the subtraction constant associated with the  $\delta'(u^2)$  singularity, which can be calculated from the nucleon-hole contribution. There is another unknown

$\delta(u^2)$  singularity. To eliminate this, we use a once subtracted dispersion relation for  $\Pi^1$ .

$$\int [\text{Im}\Pi^1(u) - \text{Im}\Pi^1(u)_{\text{pert}}(u)] u^2 e^{-u^2/M^2} du^2 = \sum_{n=2,4} \frac{(-1)^{n/2}}{(n/2-1)! M^{n+2}} b_n^1 \quad (20)$$

From a best fit analysis, one can extract the momentum dependent parameters [27]. The results are shown in Table 4.

Table 4

Results for the parameters at nuclear matter density. The values are from best fit of the Borel sum rule in eq.(20).

	$a$	$f$	$s$
Transverse $\rho$	-0.108	0.190	-0.028
Transverse $\omega$	-0.081	0.171	-0.010
Longitudinal $\rho, \omega$	0.023	0.066	0.029
Transverse $\phi$	0.004	0.010	0.009
Longitudinal $\phi$	0.009	-0.001	0.009

As discussed before, a non-vanishing  $a$  will shift the average peak position by  $\Delta M = \sqrt{m_V^2 + a\mathbf{q}^2} - m_V$ , even if there is no change in the scalar mass  $m_V$ . With the values of  $a$  obtained, we find that even at  $\mathbf{q} = .5\text{GeV}/c$ , above which point our formalism breaks down, the shifts are less than 2% (0.05 %) at nuclear matter density for the  $\rho, \omega$  ( $\phi$ ). This is smaller than the expected scalar mass shift of the  $\rho, \omega$  ( $\sim 20\%$ ) and  $\phi$  ( $\sim 3\%$ ) [28] and justifies (to a first approximation) neglecting the three momentum dependence and the polarization effect when implementing the universal scaling laws (Brown-Rho scaling) of the vector mesons in understanding the dilepton spectrum in A-A and p-A reaction[31].

The contribution of the longitudinal and transverse polarization to the dilepton spectrum, depends on the angle between the sum and difference of the three momentum of the out going dileptons[19]. However, after averaging, the contribution of the transverse polarization becomes twice that of the longitudinal polarization, as can be seen from Eq.(8). Hence, to a good approximation, one can implement the finite  $\mathbf{q}$  effect into model calculations by including only the transverse dispersion relation. Making a linear fit at the nuclear matter density, one can parameterize the vector meson mass in medium as follows,

$$\begin{aligned} \frac{m_\rho(n_n)}{m_\rho(0)} &= 1 - (0.023 \pm 0.007) \left( \frac{\mathbf{q}}{0.5} \right)^2 \frac{n_n}{n_0} \\ \frac{m_\omega(n_n)}{m_\omega(0)} &= 1 - (0.016 \pm 0.005) \left( \frac{\mathbf{q}}{0.5} \right)^2 \frac{n_n}{n_0} \\ \frac{m_\phi(n_n)}{m_\phi(0)} &= 1 + (0.0005 \pm 0.0002) \left( \frac{\mathbf{q}}{0.5} \right)^2 \frac{n_n}{n_0}, \end{aligned} \quad (21)$$

where  $\mathbf{q}$  is in the GeV unit. In a full model calculation, the effect in Eq.(21) should be added to that of Eq.(16). It should be noted that the main operators responsible for the result in Table 4 come mainly from chirally symmetric twist-2 operators. So the dispersion effect is a chirally symmetric effect and has little relation to chiral symmetry restoration.

## 4. SUMMARY

1. Chiral symmetry is restored at high temperature and/or density, while  $U_A(1)$  breaking effect persist above the transition. It would be useful to perform lattice calculations of  $U_A(1)$  breaking effect above the chiral phase transition using 2 quark-bilinear order parameter for quark flavors larger than 2.
2. Using the QCD constraints one can relate observed changes in spectral density to changes of local operators at finite temperature or density. A systematic lattice gauge theory calculations on the temperature dependence of the chiral symmetry breaking condensate would be a useful future project.
3. QCD sum rules in matter suggests that the vector meson width will increase and its peak position shift downwards in energy at finite density and temperature before it becomes part of the continuum above the critical boundary. These changes are due mainly to chiral symmetry restoration.
4. QCD sum rule in matter suggests that the dispersion effect ( finite  $\mathbf{q}$  effect) is small, but should be included in a full study of the changes in the vector meson peak in medium.

## 5. ACKNOWLEDGEMENTS

I would like to thank the organizers for the invitation to give a talk. I would like to thank T. Hatsuda for a close collaboration on the presented subject and T. D. Cohen, B. Friman and Hungchong Kim for various useful discussions.

## REFERENCES

1. D. Jido, N. Kodama, M. Oka, Phys. Rev. D **54**, 4532 (1996).
2. Su H. Lee and H. Kim, Nucl. Phys. A **612**, 418 (1997).
3. F.R. Brown *et al*, Phys. Rev. Lett. **65**, 2491 (1990).
4. Y. Iwasaki *et al*, Z. Phys. C **71**, 343 (1996).
5. T. Schäfer, hep-ph/9708256.
6. T. Wettig, T. Guhr, A. Schafer, H. A. Weidenmuller, hep-ph/9701387.
7. C. Bernard *et al*, Phys. Rev. Lett. **78**, 598 (1997).
8. G. Boyd, hep-lat/9607046.
9. G. 't Hooft, , Phys. Rev. Lett. **37**, 8 (1976); Phys. Rev. D **14**, 3432 (1976), M.A. Shifman, A.I. Vainshtein, V.I. Zakharov, Nucl. Phys. B **163**, 46 (1980).
10. Su H. Lee and T. Hatsuda, Phys. Rev. D **54**, r1871 (1996)
11. A.I. Bochkarev and M.E. Shaposhnikov, Nucl. Phys. B **268**, 220 (1986)
12. R. Pisarski, Phys. Lett. B **110**, 222 (1982)
13. H.-C. Jean, J. Piekarewicz, A.G. Williams, Phys. Rev. C **49**, 1981 (1994); H. Shiomi and T. Hatsuda, Phys. Lett. B **334**, 281 (1994).
14. K. Saito and A. W. Thomas, Phys. Rev. C **51**, 2757 (1995).
15. B. Friman, M. Soyeur, Nucl. Phys. A **600**, 477 (1996).
16. G.E. Brown and M. Rho, Phys. Rev. Lett. **66**, 2720 (1991).

17. M. Asakawa, C.M.Ko, P. Levai and X.J. Qiu, PRC **46**, 1157 (1992); G. Chanfray and P. Schuck, NPA **545**, 271 (1992); M. Herrmann, B.L.Friman and W. Nörenberg, Nucl. Phys. A **560**, 411 (1993); F. Klingl, N. Kaiser and W. Weise, Nucl. Phys. A **624**, 527 (1997).
18. B. Friman, H.J. Pirner, Nucl. Phys. A **617**, 496 (1997); R.Rapp, G. Chanfray and J. Wambach, Nucl. Phys. A **617**, 472 (1997); W. Peters *et al* nucl-th/9708004.
19. C. Gale and J. I. Kapusta, Nucl. Phys. B **357**, 65 (1991).
20. C. Song, Phys. Rev. D **48**, 1375 (1993).
21. Su H. Lee, C. Song and H. Yabu, Phys. Lett. B **341**, 407 (1995).
22. R. D. Pisarski, Phys. Rev. D **52**, 3773 (1995).
23. M. Harada and A. Shibata, Phys. Rev. D **55**, 6716 (1997).
24. K. L. Haglin, Phys. Rev. C **54**, 1492 (1996); Nucl. Phys. A **584**, 719 (1995); nucl-th/9710026.
25. C. Song, P.W. Xia and C.M. Ko, Phys. Rev. C **52**, 408 (1995).
26. T. Hatsuda, Y. Koike and Su H. Lee, Nucl. Phys. B **394**, 221 (1993).
27. Su H. Lee, nucl-th/9705048.
28. T. Hatsuda and Su H. Lee, Phys. Rev. C **46**, r34 (1992).
29. T. Hatsuda, Shiomi and Su H. Lee, Phys. Rev. C **52**, 3364 (1995).
30. S. Leupold, W. Peters and U. Mosel, nucl-th/9708016.
31. G.Q.Li, C.M. Ko and G.E.Brown, Phys. Rev. Lett. **72**, 4007 (1995).